Chemical Science

Accepted Manuscript

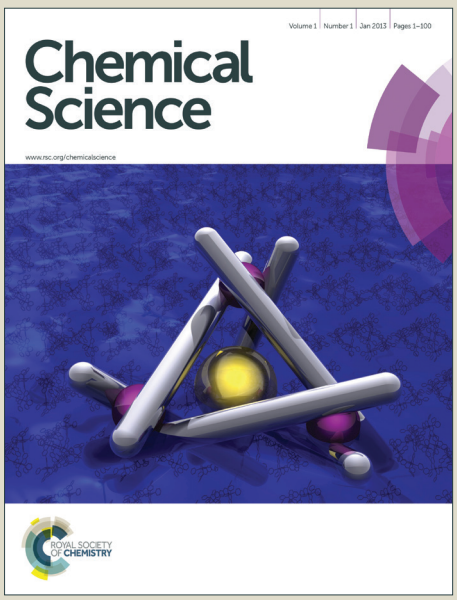

ROYAL SOCIETY OF CHEMISTRY

www.rsc.org/chemicalscience

Journal Name

RSCPublishing

ARTICLE

Helically Structured Metal-Organic Frameworks Fabricated by Using Supramolecular Assemblies as Templates

Cite this: DOI: 10.1039/x0xx00000x

Received 00th January 2012,
Accepted 00th January 2012

DOI: 10.1039/x0xx00000x

www.rsc.org/

Hui Wang,[†a] Wei Zhu,[†a] Jian Li,[a] Tian Tian,[a] Yue Lan,[a] Ning Gao,[a] Chen Wang,[a] Meng Zhang,[a] Charl F. J. Faul[b] and Guangtao Li[*a]

Controlled formation of MOF-based superstructures with well-defined nanoscale sizes and exquisite morphologies represents a big challenge, but can trigger a new set of properties distinguishing from their bulk counterparts. Here we report on the use of a self-assembled organic object to template the first example of a nanoscale helical morphology of metal-organic frameworks (MOFs). Two prototypical MOFs (**HKUST-1** and **MIL-100**) were exemplified to grow on such supramolecular assemblies. Interestingly, it was found that, dependent on the nature of precursors, not only well-defined helical MOF nanotubes could be facilely fabricated, but novel helical bundle nanostructures could also be formed. These resultant MOF superstructures show additional optical property and could be used as precursors for preparation of chiral nanocarbons.

Introduction

Metal-organic frameworks, also known as coordination polymers, are a fascinating class of hybrid porous crystalline materials made by linking metal-containing units with organic linkers using strong bonds.[1] Their unique features including high porosity, large internal surface areas, intricate porous structure, diversity and tailorable chemistry make them very attractive for numerous applications.[2] Nanoscale metal-organic frameworks (NMOFs), where the sizes of well-defined MOFs are reduced to micro- and nanoscale, show improved properties, when compared to their bulk counterparts.[3] Their potential applications can be significantly extended owing to the superior adsorption kinetics of guest species and dispersible nature that is distinct from bulk crystals.[3] Keeping these attractive features in mind, increasing efforts have been devoted to reduce the size of MOF crystals to the nanometer scale while retaining their well-defined morphologies. A few approaches, including micro-emulsion, microwave synthesis and methods using capping agents etc, have been developed for the fabrication of nanometer-sized MOFs,[3] but the nanoscale morphologies accessible to date have been largely limited to fairly basic shapes, such as nanoparticles, hollow nanospheres, nanocubes, nanorods, nanosheets, and core-shell nanostructures.[3-4] However, more complex morphologies like helices, which have promising potential applications in, for example, asymmetric catalysis, helical sensors and optical devices,[5] have not been described for MOF materials. Conceivably, controlled fabrication of hierarchical MOF-based superstructures with helical morphologies and permanent porosity would create new opportunities for the development of advanced applications owing to the combination of the intrinsic MOF properties and the nanostructure-related optical activity.

Amphiphilic molecules have long been known to self-assembly into a variety of ordered supramolecular nanostructures.[6] An intriguing aspect of amphiphiles is that the sizes, morphologies and surface chemistry of the resulting organized supramolecular assemblies are easily tunable by modulation of the molecular structure and the experimental conditions. Beyond the common micelles, vesicles and liquid crystalline mesophases, more stable and organized nanostructures such as fibers, ribbons, helices, super helices and tubes can be facilely achieved. The ability of amphiphilic molecules to form such self-assembled objects with well-defined sizes and designed morphologies implicates the great potential of supramolecular assemblies as templates for controlled production of nanostructured materials that are inaccessible by conventional methods. In this respect, the templating power of supramolecular assemblies was exemplified by transcription synthesis of metal, metal oxides, metal chalcogenides and silicates.[7] For example, Hanabusa and Shinkai reported the creation of helically nanostructured silicas by using sol-gel reaction in the presence of diaminocyclohexane-based chiral organogels.[8] Stupp et al have also successfully fabricated single and double helices of cadmium sulfide (CdS) fibers from supramolecular assemblies.[9] However, most of the

Journal Name RSCPublishing

ARTICLE

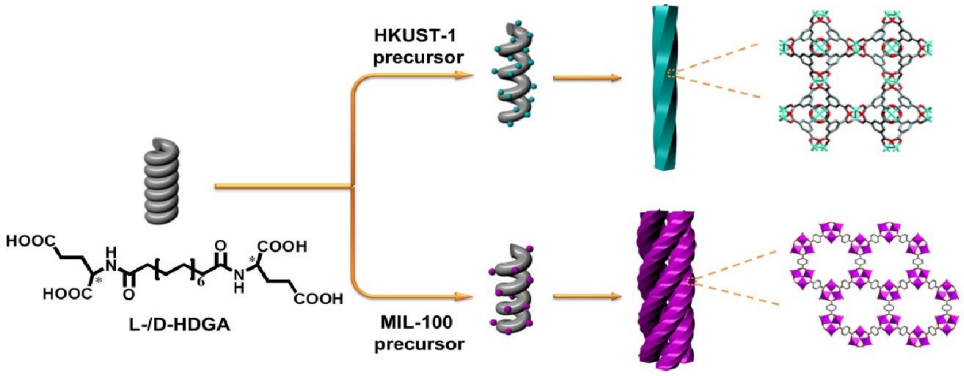

Scheme 1. Schematic illustration of the fabrication of the helical MOFs nanostructures by using supramolecular assemblies as templates.

reported works demonstrated the creation of helically nanostructured silicates, cadmium sulfide, metals and metal oxides by using supramolecular assemblies as templates.[7-9] To the best of our knowledge, there have been no reports on the direct growth of MOF crystals on the surface of discrete supramolecular assemblies to form helical MOF nanomaterials.

In this study, we therefore present the first example of the preparation of helically structured MOF nanomaterials from supramolecular assemblies of two low-molecular-weight bola-amphiphilic templates in a controlled manner. As shown in Scheme 1, two bolaamphiphiles based on D- or L-glutamic acid, respectively, were synthesized and used to form well-defined helical supramolecular aggregates. As the surface of the aggregates consists of hydrophilic carboxyl groups, it is expected that the helical surface should show a strong affinity for metal cations and thus enables the nucleation, crystallization and growth of MOFs on the curved surface of the helical aggregates. To prove our concept, a prototypical MOF (HKUST-1) was used as example. Indeed, we found that after optimization of the preparation conditions, the chirality of the helical supramolecular aggregate could be faithfully expressed onto the formed HKUST-1, affording well-defined helically nanostructured HKUST-1. D- and L-type helical NMOF products could be selectively created, depending on the chirality of the supramolecular templates used. Moreover, the pitch of the resultant helical MOFs could also be well adjusted from 170 nm to 305 nm by controlling the growth time of HKUST-1. To further examine the validity and general applicability of our controlled fabrication strategy for NMOFs with helical morphologies, another well-studied MOF (MIL-100) was also chosen to produce helical NMOF constructs under similar conditions. As expected, similar results were obtained as for HKUST-1, and nanoscale MIL-100 with a helical morphology was also produced. However, probably due to the stronger affinity of the carboxyl groups for Fe^{3+} (compared with Cu^{2+}), more complex helical bundle superstructures were achieved through intertwining of a few helical MIL-100 nanofibers. These resultant NMOF (HKUST-1 or MIL-100) superstructures showed additional optical properties and could be used as precursors for the preparation of chiral nanocarbons.

Experimental

Preparation of helical self-assembled templates

To prepare helical self-assembled templates, 2.7 mg L-HDGA solid was added into 0.5 mL pure water, sealed and heated to 100° C until fully dissolved. The solution was then cooled to room temperature and a viscous gel was formed after 10 minutes. TEM samples were prepared by suspending a portion of the L-HDGA hydrogel in H_2O, casting it onto a holey carbon coated Cu grid, and blotting off the redundant liquid with filter paper. The D-HDGA hydrogel could be fabricated and prepared for imaging in the same way.

Preparation of helical HKUST-1 (L-/D-HDGA@HKUST-1)

Typically, to prepare helical **L-HDGA@HKUST-1**, 0.5 mL L-HDGA hydrogel was diluted with 4 mL of mixed solvent (0.4 mL ethanol and 3.6 mL pure water), and stirred for 1 hour to ensure the homogeneous dispersion of self-assembled templates in mixed solution. Then 400 μL fresh MOFs precursor solution (200 μL 50 mM $Cu(NO)_3$ ethanol solution which was mixed with 200 μL 25 mM H_3BTC (1,3,5-Benzenetricarboxylic acid) ethanol solution was fed into the prepared L-HDGA

solution under magnetic stirring. After the incubation under static conditions at 26℃ for 24 h, the as-formed helical L-HDGA@HKUST-1 was collected by further centrifugation. **D-HDGA@HKUST-1** could be fabricated based on the same methodology.

n-L-HDGA@HKUST-1 (n=1, 2, 3, 4) with different shell thicknesses (from thinner to thicker: 1-L-HDGA@HKUST-1, 2-L-HDGA @HKUST-1, 3-L-HDGA@HKUST-1 and 4-L-HDGA@ HKUST-1) could be obtained by adding MOFs precursor solution dropwise. **1-L-HDGA@HKUST-1** could be fabricated by feeding 200 μL fresh MOFs precursor solution (100 μL 50 mM $Cu(NO)_3$ ethanol solution mixed with 100 μL 25 mM H_3BTC ethanol solution) into diluted L-HDGA hydrogel solution under magnetic stirring. The mixed solution was incubated under static conditions at 26℃ for 24 h. **2-L-HDGA@HKUST-1**, **3-L-HDGA@HKUST-1** and **4-L-HDGA @HKUST-1** could be obtained by repeating the procedure for **1-L-HDGA@HKUST-1** twice, three and four times. For **n-D-HDGA@HKUST-1** (n=1, 2, 3), they could be fabricated based on the same methodology with **D-HDGA** hydrogel used as template.

Preparation of helical MIL-100 (L/D-HDGA@MIL-100)

Typically, to prepare helical **L-HDGA@MIL-100**, 200 μL fresh MOFs precursor solution (100 μL 40 mM $FeCl_3$ ethanol solution mixed with 100 μL 40 mM H_3BTC ethanol solution) was fed into a diluted L-HDGA hydrogel solution under magnetic stirring, and the mixed solution was incubated under static conditions at 26℃ for 24 h. Subsequently, the procedure mentioned was repeated once more. The formed helical **L-HDGA@MIL-100** could then be collected by centrifugation. **D-HDGA@MIL-100** could be fabricated in the same way as **L-HDGA@MIL-100** except that D-HDGA hydrogel was used as template.

Preparation of helical carbon nanotubes

To prepare helical carbon nanotubes, the helical **n-L-HDGA@HKUST-1** (n=1, 2, 3) was calcined under N_2 atmosphere. The annealing procedure was performed at a heating rate of 5℃/min and kept at 600℃ for 0.5 hour, and then allowed to cooled naturally to room temperature. After that, some quantity of helical carbon nanotubes could be obtained.

Results and Discussion

L- or D-glutamic acid based bolaamphiphile (L-HDGA or D-HDGA) used here were synthesized according to a reported procedure.[10] These compounds formed helical nanotubes during self-assembly in water. Figure 1a and Figure S1 show the TEM images of the formed supramolecualr aggregates at different magnifications, which clearly indicate a single helical nanotube structure. With a pitch of about 40 nm, diameter of 16 nm and length of several micrometers, the handedness of the nanotubes is determined by the chirality of the bolaamphiphile. While L-HDGA forms right-handed helical tubes, D-HDGA forms left-handed tubes. Initially, to examine the possibility of producing

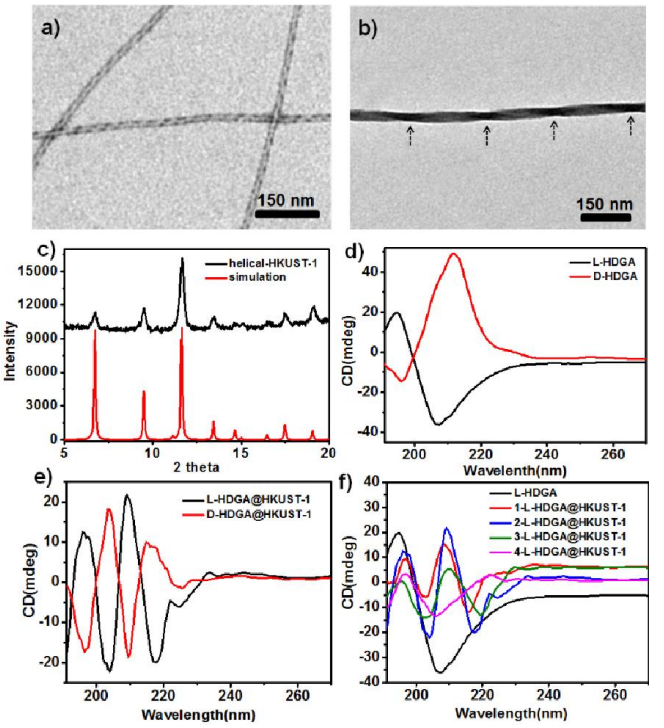

Figure 1. TEM images of right-handed helices prepared from self-assembly of L-HDGA (a) and the as-prepared right-handed helical HKUST-1 (b); XRD patterns of the resultant helical HKUST-1 and bulk HKUST-1 nanocrystals (c); CD spectra of the L-HDGA and D-HDGA based templates (d); CD spectra of the resulting right/left-handed helical HKUST-1 (e); and the evolution of the CD spectrum of the right-handed helical HKUST-1 prepared by using increased addition of MOF precursor (f).

helical MOF nanostructures by using HDGA supramolecular assemblies as templates, we added HKUST-1 precursor solution to the L-HDGA aggregates (hydrogel) system directly. After a fixed period (12 h) of crystallization and growth of HKUST-1, we found that the organized carboxyl groups on the curved surface of the formed assemblies could function as anchors to absorb metal ions for the nucleation, growth, and deposition of HKUST-1, affording MOF nanotubes. However, the formed tubes contained a lot of cracks dispersed across their surface (Figure S2), most probably because of the overlap of the HDGA assembled aggregates due to the viscous nature of the hydrogel, which hindered complete coating of MOF on the surface of the supramolecular template. We therefore decided to use a diluted suspension of HDGA aggregates in a water-ethanol mixture (instead of in the gelled state), to correctly implement the transcription of the HDGA-based template.

Hydrogels containing 0.5 wt% HDGA was first prepared and then diluted with an ethanol-water mixture to form a suspension of HDGA aggregates (see below). The addition of ethanol is favorable for the dissolution of organic ligands necessary for the formation of MOF crystals. However excess ethanol would deteriorate the inter- or intramolecular interactions (especial the hydrogen bonding) in the highly organized supramolecular aggregates, leading to the change of the formed morphology, or even the destruction of the well-defined supramolecular aggregates.[11] The evolution of the

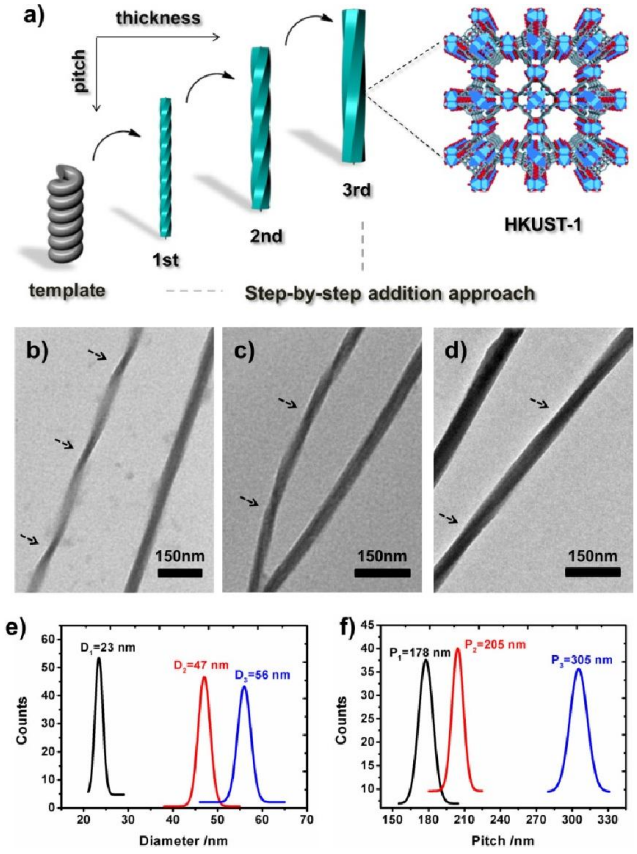

Figure 2. Schematic illustration of the fabrication of helical MOFs (HKUST-1) with different thickness and pitches based on step-by-step addition approach (a); TEM images (b-d) of the resultant helical n-L-HDGA@HKUST-1 (n=1,2,3) with increased addition of MOF precursor; the evolution of diameter (e) and pitch (f) of the resultant helical n-L-HDGA@HKUST-1 (n=1,2,3) with increased addition of MOF precursor.

supramolecular assemblies was then systematically investigated, increasing the ethanol content stepwise from 0 to 40vol %. As shown in Figure S3, the diameters of the HDGA nanotubes become larger, and the pitch of helical tubes become larger with the gradual increase of ethanol content in the mixture. Based on this result, a water-ethanol mixture containing 10 vol% ethanol was used to dilute the HDGA hydrogel. The MOF nanomaterial (L-HDGA@HKUST-1) was successfully fabricated under this conditions, showing well-defined sizes and the exquisite helical morphology. Figure 1b shows a representative TEM image of the as-prepared L-HDGA@HKUST-1, displaying a distinctive right-handed helical structure, which is consistent with the chirality of the L-HDGA templates used. The outer diameter of the as-prepared MOF helix was 40 nm and the pitch of outer surface along the rod axis was estimated to be approximately 200 nm, as indicated by the arrows. The crystal structure of the HKUST-1 deposited on the L-HDGA-based aggregates was confirmed by power X-ray diffraction (Figure 1c).[12] Consistent with the TEM observation, the chiral conformations of the D-/L-HDGA templates and the resulting helical D-/L-HDGA@HKUST-1 were clearly detected using a circular dichroism (CD) spectrometer (Figure 1d-e). In the case of the diluted L-HDGA hydrogel suspension, a positive and negative Cotton effect was observed at 195 nm and 205 nm, respectively, with a crossover at 198 nm, which is close to the absorption band of the L-HDGA (Figure S4a). However, for the sample of L-HDGA@HKUST-1, a new exciton-coupling band was detected in the range of 205-235 nm with a crossover at 213 nm, which is assigned to a ligand-to-metal charge transfer (LMCT) transition from BTC^{3-} to Cu^{2+}.[13] This result indicates that the deposited HKUST-1, which possesses an achiral framework, inherits the chirality of the helical template and so shows CD activity in the ultraviolet wavelength region.

It should be noted that the conventional MOF HKUST-1 microcrystal exhibits two absorption bands: the ligand-to-metal charge transfer transition (LMCT) with an edge around 280 nm and the d-d transition of the Cu^{2+} at ca. 750 nm (Figure S4b).[13,14] Unfortunately, we found that the formed helical HKUST-1 nanowires dispersed in water-ethanol mixture only show the LMCT (Figure S4a). However, the absorption band associated with d-d transition of Cu^{2+} at visual light region is too weak to be detectable. The exact reason is still not clear. The possible mechanism behind this phenomenon is due to the coordination of some solvent molecules in axial direction of the metal (Cu^{2+}), which induces the enhancement of the symmetry around copper. As a result, the molar absorptivity (ε) associated with d-d transition of Cu^{2+} was significantly reduced.[13,14] In fact, we also found the suspension of the conventional HKUST-1 nanocrystals in water-ethanol mixture didn't exhibit the absorption band associated with d-d transition of Cu^{2+} at visual light region (Figure S4a). Thus, the CD signal corresponding to this absorbance band (d-d transition of Cu^{2+}) in the visible-light region is absent for the suspension of the formed helical MOF wires. Similar results were also observed for the case of D-HDGA@HKUST-1. As shown in Figure 1d-e, the mirror-imaged CD signals clearly confirmed the antipodal left- and right-handed helical templates (Figure 1d) and the resulting helical MOFs (Figure 1e) with enantiomeric morphologies.

In our work, the helical MOF wires were prepared in a diluted suspension of the formed supramolecular assemblies. The increase of the concentration of the supramolecular assemblies or MOF precursor could lead to ill-defined MOF wire products or massive MOF nanocrystals due to the competition growth of MOF in bulk solution. At present, it is still difficult to produce enough amount of helical MOF wires for corresponding measurements in the solid samples. Now we are focused on the development of new method or approach to solve the mentioned problem. We hope that in near future we could make the UV-vis and CD spectral measurements of the helical MOF wires in the solid samples, which are expected to produce the signals in visual light region.

To fine tune the morphology of the final products, a step-by-step addition approach of fresh HKUST-1 precursor solution into a suspension of HDGA aggregates was employed. As shown in Figure 2, with the stepwise addition of HKUST-1 precursor, the diameters of the resultant L-HDGA@HKUST-1 gradually increased from 23 nm to 56 nm, and the pitches of the corresponding products varied from 178 nm to 305 nm. In our

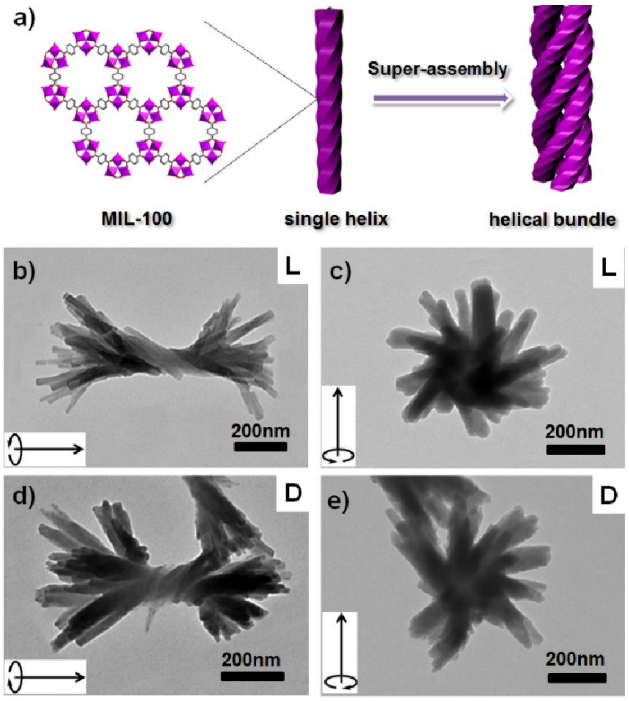

Figure 3. Schematic illustration of the formation of hierarchical superstructure (a); TEM images of the resulting right-handed (b, c) and left-handed (d, e) hierarchical MIL-100 superstructures. The arrow in Insect of each SEM image is for assisting identification of the direction of the helicity of the formed superstructure

case, all the diameters and pitches were measured from TEM images manually. These results indicate that by controlling the amount of MOF precursor added into the suspension of templates, the thickness and pitch of the resultant MOF nanomaterials can be finely adjusted. Helical MOF nanotubes with thick wall could be facilely fabricated using this approach, which might prevent the collapse of NMOFs during the removal of organic templates and provides opportunities for further practical use. Similar to the case of L-HDGA, by using D-HDGA aggregates as templates, helical D-HDGA@HKUST-1 with exclusively left- handed chirality was also obtained (Figure S8). These structures, from D-HDGA templates, are mirror images of the helical L-HDGA@HKUST-1 nanostructures. A series of left-handed helical HKUST-1 MOFs with different thickness and pitches were achieved through a similar procedure as described above (Figure S8).

To reveal the evolution of the helical NMOFs, circular dichroism spectrometry was used to detect the LMCT transition during the formation process. As shown in Figure 1f, with the stepwise addition of HKUST-1 precursor into the L-HDGA template suspension, the CD signal of L-HDGA templates decreased gradually, while the CD signal assigned to LMCT transition from BTC^{3-} to Cu^{2+} enhanced at the first two addition procedure. This enhanced absorption of LMCT process (Figure S6) could attribute to the increased thickness of MOF shells. With the further addition of HKUST-1 precursor, the pitches of the resulting helical MOF got longer and finally disappeared (Figure 2d and Figure S5), resulting in the CD signals assigned to LMCT transition being weakened and/or disappeared. Figure S6 and Figure S7 show the evolution of the UV-vis spectra of the reaction system with different MOF precursor concentrations and deposition time of MOF crystals, respectively. It is found that in both cases the absorption band of the as-prepared helical MOF nanowires only changed their intensity, while the location remains unchanged. This result indicates that the coordination of the carboxylate of template surface with metal ions hardly exerts a marked influence on the structure of the deposited MOF materials. The MOF deposited on template surface has the same structure as that of the conventional MOF. Thus, the LMCT and d-d transitions variations within the helical conformation were not detected in our case.

The preferred affinity of metal ions (Cu^{2+}) for the carboxyl groups of the organized HDGA assembled surface, which serves to initiate nucleation and subsequent growth of the MOFs along the curved assemble surface is believed to be responsible for the formation of the observed helical NMOFs. However, as shown in Figure 2b-d, the pitches of all products are clearly longer than those of their HDGA templates. To gain insight into the formation of helical MOF nanotubes under the chosen reaction conditions, aqueous solution containing different amounts of ethanol (0, 10, 20 and 30 vol%) were added to the L-HDGA hydrogel, respectively. CD measurements were performed on the resultant suspensions to reveal the change of the molecular packing of the self-assembled templates. It was found that with the increased concentration of ethanol the CD signal intensity of L-HDGA-based supramolecular aggregates decreased gradually (Figure S9). This result implies that the presence of ethanol could influence the inter- or intramolecular interactions (especial the hydrogen bonding) of the HDGA assembled aggregates, loosening molecular packing of amphiphiles and stretching the pitch of HDGA helical tubes in the water-ethanol solution. Thus, compared with the dried samples for TEM observation, the supramolecular templates suspended in water-ethanol solution should have longer pitches. Additionally, the nucleation and growth of MOF nanocrystals will probably fill up the space between the helices, leading to further broadening of the pitch of the formed helical NMOFs.

To demonstrate the "template" effect of HDGA supramolecular aggregates, a high polarity solvent (methanol) was chosen to remove the HDGA assemblies from the as-prepared helical products. It should be noted that for the case of products with a thin MOF shell, the removal of template caused the collapse of the MOF superstructures. However, for the products with a thicker MOF shell the HDGA template could be removed in methanol within a few minutes, yielding nanotubes with a helical morphology (Figure S10). The inner diameter of the nanotubes is approximately 18 nm, which is consistent with the diameter of the used HDGA helical aggregates. This result clearly shows the templating effect of HDGA assemblies for the formation of helical NMOFs.

To further demonstrate the validity and general applicability of the above mentioned transcription scheme, another

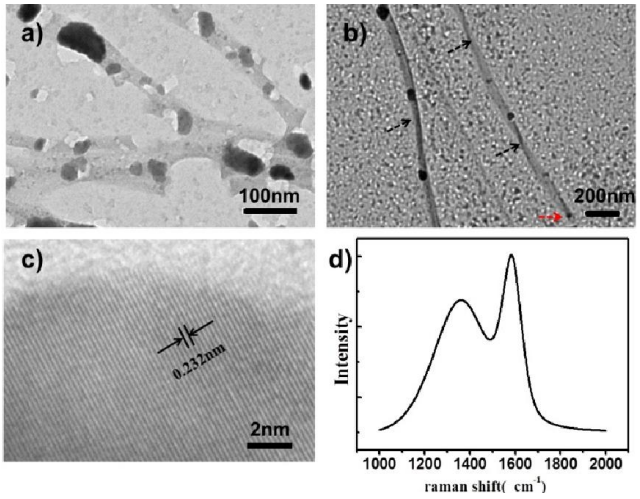

Figure 4. TEM images of the carbon nanostructures produced from L-HDGA@HKUST-1 with thin (a) and thick (b) MOF shell; (c) HR-TEM image of the Cu nanoparticles decorated on carbon surface; (d) Raman spectrum of the resultant carbon materials.

prototypical MOF (MIL-100) was chosen for producing MIL-100 based helices. A procedure similar to that of the helical HKUST-1 was adopted with the exception that $FeCl_3 \cdot 6H_2O$ instead of $Cu(NO_3)_2$ was used in the preparation. Similar phenomena and results were observed. The seeding and subsequent growth of MIL-100 on the surface of L- or D-HDGA based supramolecular aggregates afforded a large number of single helical MIL-100 nanostructures (Figure S11). Interestingly, the well-defined helical MIL-100 nano-objects could further self-assemble to form bundles of helical nanostructures exhibiting a further higher level of organization (Figure 3), most probably due to the high coordinational valence and high affinity of Fe^{3+} relative to Cu^{2+}. We furthermore found that the formed hierarchical superstructures inherited the chirality of their HDGA templates at different length scales, as shown in Figure 3b-c and Figure 3d-e. At present the formation mechanism of these hierarchical superstructures is still not clear. Nevertheless the obtained findings have already shown the power of the supramolecular aggregate transcription strategy for efficiently accessing NMOFs with novel morphologies.

Helically nanostructured carbons have attracted great attention owing to their unique elasticity, chirality, and electromagnetic wave absorption properties. However, efficient production of enantiomerically pure carbon samples remains a big challenge.[15] Very recently, MOFs have been demonstrated as novel precursors to form carbon nanomaterials.[16] Inspired by these reports, we attempted to utilize our prepared NMOFs with helical structure as precursors to fabricate helical nanocarbons. As demonstration, L-HDGA @HKUST-1 with different thicknesses of MOF shells were carbonized at 600°C under an inert N_2 atmosphere for 30 min. Figure 4 shows TEM images of the resultant products. For samples with thin HKUST-1 shell, only poorly defined perforated carbon nanostructures were obtained, as the thin shell of the L-HDGA/HKUST-1 NMOF was not robust enough to maintain its morphology during carbonization (Figure 4a). However, when L-HDGA/HKUST-1 samples with thick MOF shell was used for carbonization, well-defined nanotubes with exclusively right-handed morphologies were obtained (Figure 4b). Additionally, during the carbonization process at high temperature, the Cu^{2+} ions in HKUST-1 could be reduced to copper nanoparticles with size around 20 nm (Figure 4c).[16b] Clearly, Figure 4c showed the typical lattice fringes of the copper metal. As a clear evidence for the formation of carbon nanostructures, Raman spectra for all products exhibited D and G bands at 1345 cm^{-1} and 1588 cm^{-1} (Figure 4d), which are associated with the presence of disordered and graphitic carbon structure, respectively.[17]

The preliminary results described above are encouraging. Although this new transcription scheme was tested with HKUST-1 and MIL-100, it can, in principle, be used as a general and effective transcription scheme for creating various nanostructured MOFs with well-defined morphologies. In this works, probably owing to the use of helical nanotubes as template, the resultant NMOF helices are not remarkable when compared to that of the supramolecular templates. However, we believe MOF-based nanomaterials with more exquisite helical morphology should be substantially achieved, when helical fibers are utilized for transcription. This part of work is still ongoing in our lab. Over the past few decades the research area of fabrication of the organized supramolecular assemblies in a controlled fashion has matured. A rich variety of discrete assemblies with well-defined sizes and novel morphologies have been achieved by modulation of the molecular structure of the amphiphiles and the assembly conditions.[6] Not only carboxyl groups but also N-containing or amino acid units, that are very beneficial for anchoring MOFmaterials,[18] could be used as head groups for the development of amphiphilic molecules. These results and knowledge could enable the construction of novel NMOF superstructures inaccessible by conventional methods.

Conclusion

In summary, we report the first example of nanoscale metal-organic frameworks with helical morphologies that may have interesting future optical and chemical sensing applications. Perhaps more importantly, this work represents a step towards the goal of harnessing the power of organized supramolecular aggregates to construct MOF superstructures with well-defined nanoscale features and exquisite morphologies, beyond what has been accomplished by using conventional methods. Our results suggest that by using appropriate supramolecular nanoobjects one can achieve efficient control of the morphology of the templated MOF materials. In view of the virtually unlimited tunability of supramolecular assemblies, we believe more complicated MOF nano- or superstructures should be accessible with this approach, which can significantly extend the applications of MOFs by exploiting size and morphology related properties.

Acknowledgements

We gratefully acknowledge the financial support from the NSF China (21025311, 21121004, and 91027016), MOST Programs (2011CB808403 and 2013CB834502) and the Deutsche Forschungsgemeinschaft DFG (TRR61).

Notes and references

[a]*Department of Chemistry and Key Lab of Organic Optoelectronics & Molecular Engineering, Tsinghua University,*
Beijing, 100084 (P. R. China)
Tel: 86-010-62792905;
E-mail: lgt@mail.tsinghua.edu.cn
[b]*School of Chemistry, University of Bristol, Cantock's Close, Bristol BS8 1TS, U. K.*

† These authors contributed equally to this work. Electronic Supplementary Information (ESI) available: [Detailed TEM images and other extensive figures]. See DOI: 10.1039/b000000x/

1 a) H. C. Zhou, J. R. Long and O. M. Yaghi, *Chem. Rev.*, 2012, **112**, 673; b) J. R. Long and O. M. Yaghi, *Chem. Soc. Rev.*, 2009, **38**, 1213.

2 a) H. Furukawa, K. E. Cordova, M. O'Keeffe and O. M. Yaghi, *Science.,* 2013, **341**, 1230444; b) C. Wang, D. Liu, and W. Lin, *J. Am. Chem. Soc.,* 2013, **135**, 13222; c) R. Matsuda, T. Tsujino, H. Sato, Y. Kubota, K. Morishige, M. Takata and S. Kitagawa, *Chem. Sci*., 2010, **1**, 315; d) Z. H. Hu, C. A. Tao, H. P. Liu, X. R. Zou, H. Zhu and J. F. Wang, *J. Mater. Chem. A*.2014, **2**, 14222.

3 a)J. D.Rocca, D.Liu, and W.Lin, *Acc. Chem. Res*., 2011, **44**, 957; b) A. Carne, C. Carbonell, I. Imaz, and D. Maspoch, *Chem. Soc. Rev.*, 2011, **40**, 291; c) E. A. Fluegel, A. Ranft, F. Haase and B. V. Lotsch, *J. Mater. Chem.*, 2012, **22**, 10133.

4 a) R. Ameloot, F. Vermoortele, W. Vanhove, M. B. J. Roeffaers, B. F. Sels and D. E.De Vos, *Nat. Chem.,* 2011, **3**, 382; b) W. Cho, H. J. Lee and M. Oh, *J. Am. Chem. Soc.,* 2008, **130**, 16943; c) J. Son, H. J. Lee and M. Oh, *Chem. Eur. J.,* 2013, **19**, 6546; d) P. Z. Li, Y. Maeda and Q. Xu, *Chem. Commun.,* 2011, **47**, 8436; e) Y. S. Li, H. Bux, A. Feldhoff, G. L. Li, W. S. Yang and J. Caro, *Adv. Mater.*, 2010, **22**, 3322.

5 J. H. Jung, M. Park and S. Shinkai, *Chem. Soc. Rev.,* 2010, **39**, 4286.

6 a) A. Sorrenti, O. Illa and R. M. Ortuño, *Chem. Soc. Rev.,* 2013, **42**, 8200; b) T. Shimizu, M. Masuda and H. Minamikawa, *Chem. Rev.,*2005, **105,** 1401; c) J.-H. Fuhrhop and T. Wang, *Chem. Rev.* 2004, **104**, 2901; c) G.-L. Wu, J. Thomas, M. Smet, Z.-Q.Wang and X. Zhang, *Chem. Sci.*, 2014, **5**, 3267.

7 a) H. B. Qiu and S. A. Che, *Chem. Soc. Rev.*, 2011, **40**, 1259; b) Y. Liu, J. Goebl andY. Yin, *Chem. Soc. Rev.,* 2013, **42**, 2610; c) Y. Wang, J. Xu, Y. W. Wang and H. Y. Chen, *Chem. Soc. Rev*., 2013, **42**, 2930; d) Y. Yao, M. Xue, Z.-B. Zhang, M.-M. Zhang, Y. Wang and F.-H. Huang, *Chem. Sci*., 2013, **4**, 3667.

8 a) S. Kobayashi, N. Hamasaki, M. Suzuki, M. Kimura, H. Shirai and K. Hanabusa, *J. Am. Chem. Soc.*, 2002, **124**, 6550; b) J. H. Jung, Y. Ono, K. Hanabusa and S. Shinkai, *J. Am. Chem. Soc.,*2000, **122**,5008.

9 a) E. D. Sone, E. R. Zubarev and S. I. Stupp, *Angew. Chem.,* 2002, **114**, 1781; *Angew. Chem., Int. Ed.,* 2002, **41**, 1705; b) E. D. Sone, E. RZubarev, and S. I. Stupp, *Small.,* 2005, **1**, 694.

10 a) P. Gao, C. L. Zhan and M. H. Liu, *Langmuir.,* 2006, **22**, 775； b) J. Jiang, T. Y. Wang and M. H. Liu, *Chem.Comm.,* 2010, **46**, 7178.

11 a) P. Gao, C. L. Zhan, L. Z. Liu, Y.-B.Zhou and M.H.Liu, *Chem. Commun.*, 2004, **10**, 1174; b) M. S. Spector, J. V.Selinger and J. M.Schnur, *J. Am. Chem. Soc.*, 1997,**119**, 8533.

12 S. S. Y. Chui, S. M. F. Lo, J. P. H. Charmant, A. G. Orpen and I. D. Williams, *Science*., 1999, **283**, 1148.

13 C. Prestipino, L. Regli, J. G.Vitillo, F. Bonino, A. Damin, C. Lamberti, A. Zecchina, P. L. Solari, K. O. Kongshaug and S. Bordiga, *Chem. Mater.,* 2006,**18**,1337.

14 E. Borfecchia, S. Maurelli, D. Gianolio, E. Groppo, M. Chiesa, F. Bonino and C. Lamberti, *J. Phys. Chem. C,* 2012, **116**, 19839.

15 S. H. Liu, Y. Y. Duan, X. J. Feng, J. Yang and S. N. Che, *Angew. Che.*, 2013, **125**, 6996; *Angew. Chem. Int. Ed.,* 2013, **52**, 6858.

16 a) H. L. Jiang, B. Liu, Y. Q. Lan, K. Kuratani, T. Akita, H. Shioyama, F. Q. Zong and Q. Xu, *J. Am. Chem. Soc.*, 2011, **133**, 11854; b) R. Das, P. Pachfule, R. Banerjee and P. Poddar, *Nanoscale.,* 2012, **4**, 591; c) P.-P. Su, H. Xiao, J. Zhao, Y. Yao, Z.-G. Shao, C. Li and Q.-H. Yang, *Chem. Sci.*,2013, 4, 2941.

17 Q. Wang, W. Xia, W. Guo, L. An, D. Xia andR. Zou, *Chem. Asian. J.*, 2013, **8**, 1879.

18 D. Zacher, R. Schmid, C. Wöll and R. A. Fischer, *Angew. Chem.*, 2011, **123**, 184; *Angew. Chem. Int. Ed.,* 2011, **50**, 176.